Cambridge University Press
978-0-521-81750-9 - Pattern Formation: An Introduction to Methods
Rebecca B. Hoyle
Excerpt
More information

1

What are natural patterns?

This book is about patterns: stripes on tigers, whorls in your fingerprints, ripples in sandy deserts, and hexagons you can cook in your own kitchen. More precisely it will be concerned with fairly regular spatial or spatiotemporal patterns that are seen in natural systems – deserts, fingertips, animal coats, stars – and in laboratory or kitchen experiments. These are structures you can pick out by eye as being special in some way, typically periodic in space (Figure 1.1), at least locally. The most common are stripes, squares and hexagons – periodic patterns that tesselate the plane – and rotating spirals or pulsating targets. Quasipatterns with twelvefold rotational symmetry (Figure 1.2) never repeat in any direction, but they look regular at a casual glance, while spiral defect chaos (Figure 1.3) is disordered on a large scale, but locally its constituent moving spirals and patches of stripes are spatially periodic.

Similar patterns are seen in wildly different natural contexts: for example, zebra stripes, desert sand ripples, granular segregation patterns and convection rolls all look stripy, and they even share the same dislocation defects, where two stripes merge into one (Figure 1.4). Rotating spirals appear in a dish of reacting chemicals and in an arrhythmic human heart. Squares crop up in convection and in a layer of vibrated sand. It turns out to be common for a given pattern to show up in several different systems, and for many aspects of its behaviour to be independent of the small details of its environment. This has led to a symmetry-based approach to the description of pattern formation: from this point of view, patterns are universal, and we can find out nearly everything we need to know about them using only their symmetries and those of their surroundings.

This book is intended as an introduction to these symmetry-based techniques and their relationship with more traditional modelling approaches. Before starting on the universal, however, I am going to talk a bit about the specific, describing the archetypal pattern-forming systems: convection, reaction-diffusion and the Faraday wave experiment.

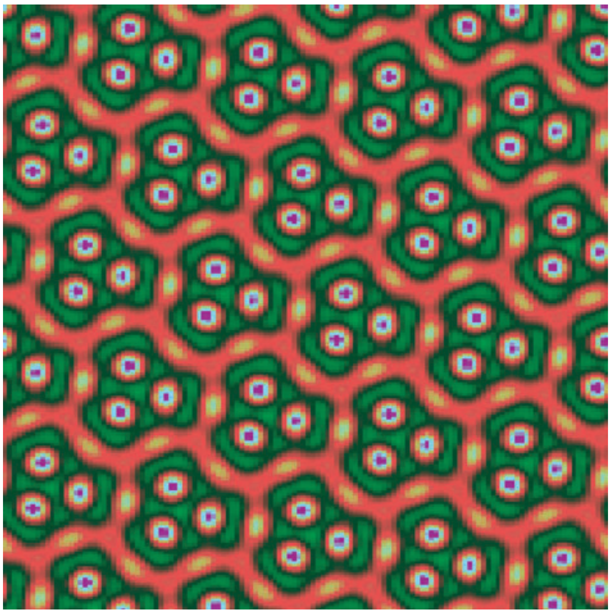

Fig. 1.1. A periodic super triangle pattern that tesselates the plane. Super triangles can be seen in Faraday wave experiments – see Sections 1.3 and 6.1 and also Silber and Proctor (1998) and Kudrolli, Pier and Gollub (1998). Image courtesy of and ©Mary Silber, Northwestern University, 2003.

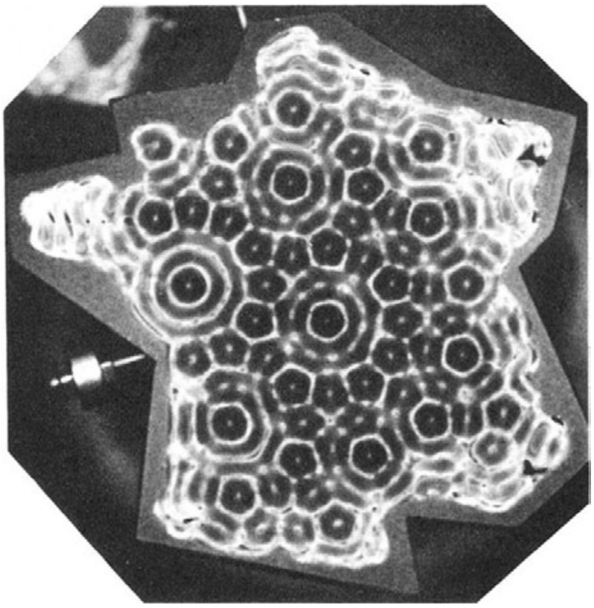

Fig. 1.2. Quasipatterns in a Faraday wave experiment. The experimenters chose a container in the shape of France to show that the quasipattern was not caused by boundary effects. Reprinted with permission from W. S. Edwards and S. Fauve, *Physical Review E*, **47**, R788, 1993. ©American Physical Society, 1993.

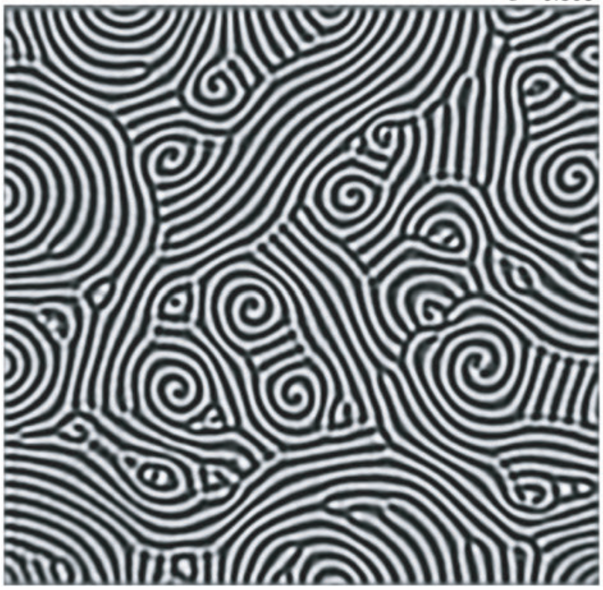

Fig. 1.3. Spiral defect chaos in a Rayleigh–Bénard convection experiment. Image courtesy of and ©Nonlinear Phenomena Group, LASSP, Cornell University, August 2004.

Many of the mathematical techniques and ideas I shall touch upon here are revisited in greater detail in subsequent chapters, so don't worry if you don't follow every step on a first reading. It is enough to get a flavour of the applications to which the theory of pattern formation is relevant. If you are not familiar with simple bifurcation theory it may help to read through the basic ideas in Chapter 2 before attempting to follow the details of the calculations. Simple vector calculus is also needed here, and occasionally in the rest of the book. The descriptions of the phenomena themselves, however, require no particular background knowledge.

Throughout the book I shall use bold italic font for vectors, $\boldsymbol{v}$, but standard italic font for vector-valued functions, $f(t) = \boldsymbol{v}$, and for matrices, scalars and scalar-valued functions.

1.1 Convection

A huge proportion of the early work on pattern formation was motivated by the study of **convection**, which is the overturning of a fluid that is heated from below. Heat at the bottom of a container causes the fluid there to expand, become less dense and more buoyant and so to rise through the colder fluid above. As the

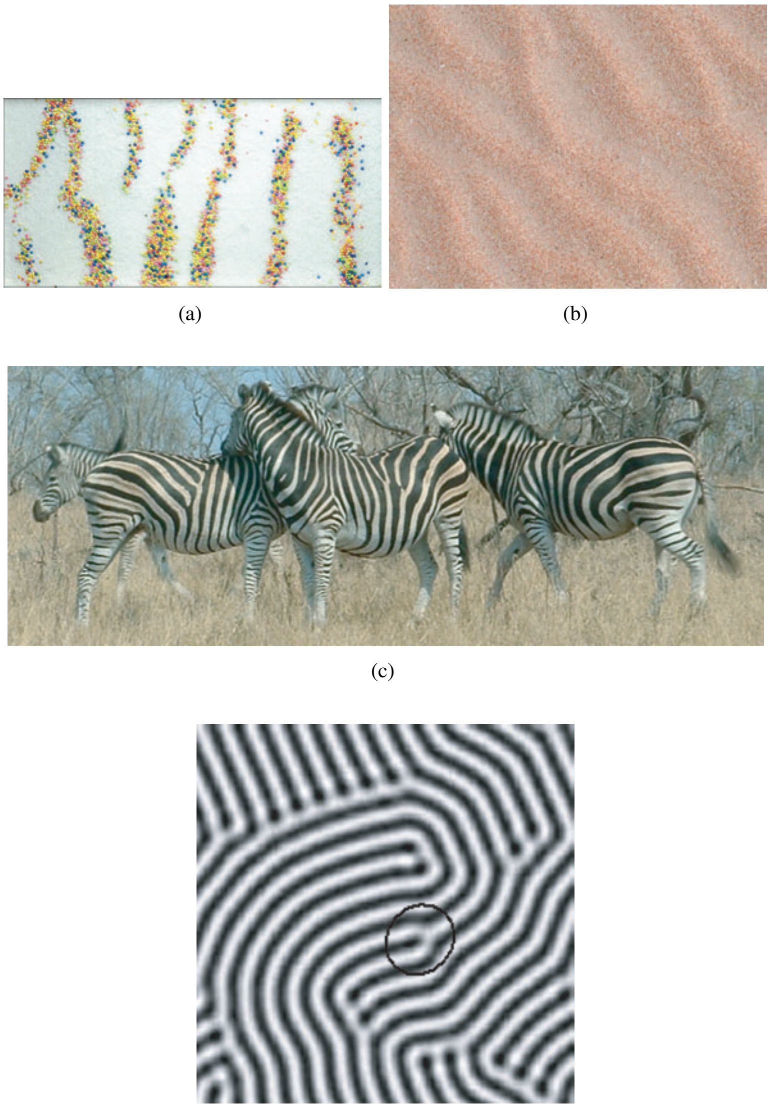

(a) (b) (c) (d)

Fig. 1.4. Stripe patterns showing dislocations, where two stripes merge into one: (a) segregation in a layer of horizontally shaken sugar and hundreds and thousands (otherwise known as sprinkles or cake decorations); (b) sand ripples in the Sahara desert; (c) on zebras (courtesy of and ©Ed Webb, 2004), and (d) in a numerical simulation of the Swift–Hohenberg convection model. Image (a) reprinted with permission from Mullin, T., *Science* **295**, 1851 (2002). ©AAAS (2002).

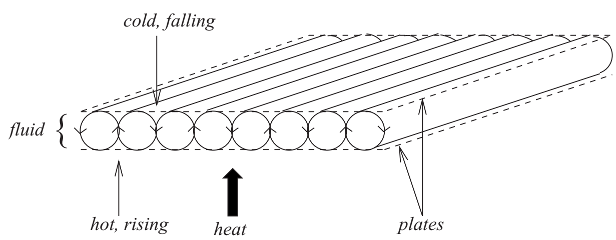

Fig. 1.5. The rise and fall of fluid in convection creates patterns, such as the rolls or stripes shown here. Arrows show the direction of fluid movement. The pattern looks like stripes when observed from the top.

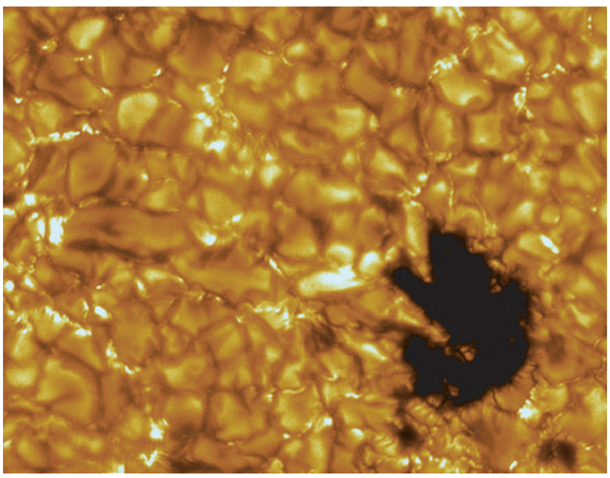

Fig. 1.6. Convection cells in the photosphere of the Sun (solar granulation). The dark region is a sunspot. Image courtesy of and ©Dr Tom Berger, Lockheed Martin Solar and Astrophysics Lab, Palo Alto, California, 2003.

fluid rises away from the heat source, it cools, becoming denser than the fluid below, and so falls back down to the bottom of the container under the influence of gravity (Figure 1.5). The cycle then repeats, so the fluid is constantly overturning. The rising and falling fluid forms spatial patterns, most commonly **stripes** or **convection rolls** (Figure 1.5), though more complicated patterns such as hexagons and squares are also possible, depending on the details of the physical system and the fluid properties. Convection is often investigated through carefully designed laboratory experiments, but the reason it is so important and has been studied so extensively is that convection occurs naturally in the environment: in the Earth's mantle, convection leads to the movement of tectonic plates or 'continental drift'; in the oceans it drives circulations such as the Gulf Stream that keeps northwestern Europe so much warmer than its northern latitudes would suggest; in the atmosphere, convection creates thunderclouds and in stars, such as the Sun (Figure 1.6), convection transports energy efficiently from the core where it is produced to the surface where it is released.

In the laboratory, the pattern or **planform** is typically visualised using the **shadowgraph** technique. In this method, a light is shone down onto the convection cell, which must have a transparent top plate and a reflective bottom plate. The warm rising fluid has a lower index of refraction than the cold falling fluid, and so the light is focused towards the cold regions, which appear bright, while the warmer regions remain dark. The pattern can be seen reflected off the bottom plate. Other methods of visualisation are possible, as we shall see in the following kitchen experiment.

1.1.1 How to cook hexagons in your own kitchen

I used to think that apart from stripes, which you can clearly see in fingerprints and on zebras and so on, natural patterns were actually quite exotic – only to be found on the surface of the Sun, and in labs where long hours had been spent in perfecting the experimental set-up. Then I learned how to cook hexagons using only a frying pan, some cooking oil and a sprinkling of pepper.

Cooked hexagons

Warning: This recipe involves hot oil, which is potentially quite dangerous. Only competent adult cooks should attempt to cook hexagons. Do not let any water get into the oil. If the oil starts to smoke, remove the pan from the heat immediately.

(i) Put a little cooking oil into a flat-bottomed cooking pan. A depth of 0.5–1.00 mm is adequate. You will be able to see the hexagons more easily if the inside of the bottom of the pan is a pale colour. Copper-bottomed pans make the best hexagons because they conduct heat well.
(ii) Mix some very finely ground black pepper or other coloured spice into the oil for visualisation purposes. There should be enough pepper or spice to finely coat the bottom of the pan.
(iii) Put the pan on a flat even heat source – an old-fashioned oil- or coal-fired stove with solid flat plates is best. Gas or electric rings will also work, but the hexagons will be less regular because the heat will be more localised and because the pan is likely to be tilted a bit.
(iv) Heat very gently. Do not let the oil get very hot. A few seconds' heating should be adequate. (Let the hot plate or electric ring heat up first before you put the pan of oil on it.)
(v) Look sideways at the surface of the oil: you should see hexagon-shaped dimples as the oil heats up and starts to convect. You should also see pepper or spice swept along the bottom of the pan into little heaps arranged approximately hexagonally. Once the

Cambridge University Press
978-0-521-81750-9 - Pattern Formation: An Introduction to Methods
Rebecca B. Hoyle
Excerpt
More information

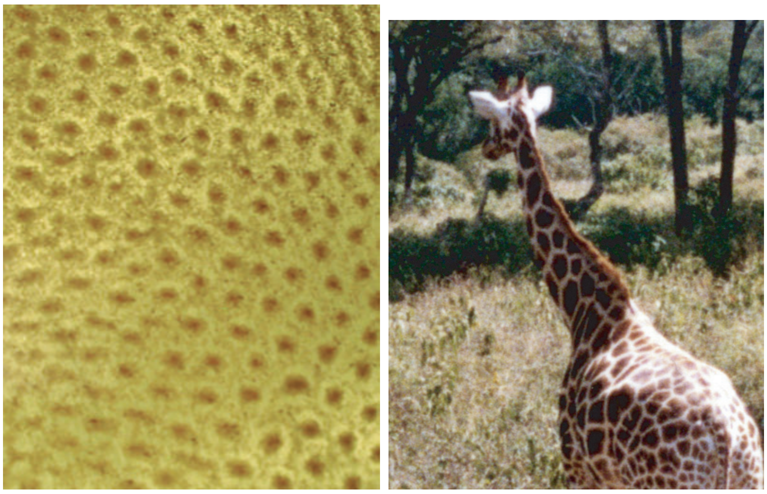

(a) (b)

Fig. 1.7. Irregular hexagonal patterns in (a) heated cooking oil, and (b) a giraffe's coat markings. Cooked hexagon image courtesy of and ©Nick Safford, 2004.

hexagons have formed, the heaps of spice should remain visible if you remove the pan carefully from the heat. In any case, you should not continue to heat the oil for more than a few seconds.

(vi) If your hexagons go wrong, take the pan off the heat, cool it down and start again. The hexagons come out best if the oil is cool to start with, and should be seen within a few seconds of heating.

Figure 1.7a shows some hexagons cooked using turmeric for visualisation. You can just about see the cell boundaries around each central blob of turmeric. The hexagons are pretty irregular, since this is not a highly controlled experiment. In fact you are likely to see as many pentagons and heptagons as hexagons; giraffe markings also show irregular hexagonal patterns like these (Figure 1.7b). It is also typical to see stripes in the heated oil if the pan is not quite horizontal and the oil is flowing downhill under gravity in places.

1.1.2 Governing equations for Rayleigh–Bénard convection in the Oberbeck–Boussinesq approximation

In 1916, Lord Rayleigh published a paper analysing convection experiments carried out by Henri Bénard and published in 1900. In fact Rayleigh's theory described convection in a fluid that completely fills the gap between the top and bottom plates of a closed cell, whereas Bénard's experiments had used a container that was open at the top so that the fluid had a free surface. These two situations are

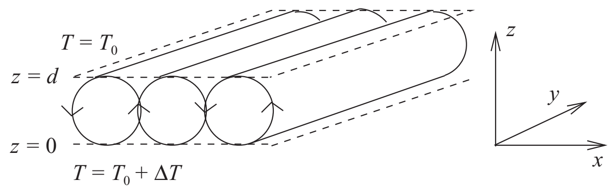

Fig. 1.8. Diagram of the convection system described by equations (1.2) and (1.3). The fluid fills the gap between two horizontal plates at $z = 0$ and d. The top plate is maintained at a temperature $T = T_0$, while the temperature at the bottom is heated to a temperature $T = T_0 + \Delta T$, where $\Delta T > 0$.

actually quite different, because in a filled closed cell buoyancy changes alone are responsible for convection, whereas if the top is open, temperature-induced variations in the surface tension can also drive the motion. Convection between two horizontal plates is known as **Rayleigh–Bénard** or simply **Bénard** convection, while the free surface case is called **Bénard–Marangoni** convection. In his 1958 paper on surface-tension-driven convection Pearson introduced a dimensionless number that measures the relative effects of surface tension and viscous forces; this was later named the Marangoni number after a nineteenth-century Italian scientist, Carlo Marangoni, who noted that fluid flow is coupled to surface tension.

This section will set out the equations used to describe Rayleigh–Bénard convection and show that rolls or stripes are an approximate solution close to onset.

Consider a layer of fluid between two plates at $z = 0$ and d, heated uniformly from below, with the top plate held at a temperature $T = T_0$ and the bottom plate at the higher temperature $T = T_0 + \Delta T$, where ΔT is positive, as shown in Figure 1.8. We assume that the fluid density, ρ, varies linearly with the temperature, T, so that

$$\rho = \rho_0[1 - \alpha(T - T_0)], \tag{1.1}$$

where ρ_0 is the fluid density at $T = T_0$ and α is the (constant) coefficient of thermal expansion, and we further assume that the density variation is only significant in the buoyancy force: this is the **Oberbeck–Boussinesq approximation**. These assumptions are incorporated into the **Navier–Stokes equation** for fluid flow, the heat equation and the continuity equation, to give

$$\rho_0\left(\frac{\partial \boldsymbol{u}}{\partial t} + (\boldsymbol{u}\cdot\nabla)\boldsymbol{u}\right) = -\nabla p - \rho g\widehat{\boldsymbol{z}} + \rho_0\nu\nabla^2\boldsymbol{u}, \tag{1.2}$$

$$\frac{\partial T}{\partial t} + (\boldsymbol{u}\cdot\nabla)T = \kappa\nabla^2 T, \tag{1.3}$$

$$\nabla\cdot\boldsymbol{u} = 0, \tag{1.4}$$

Cambridge University Press
978-0-521-81750-9 - Pattern Formation: An Introduction to Methods
Rebecca B. Hoyle
Excerpt
More information

where $\boldsymbol{u}(x, y, z, t) \in \mathbb{R}^3$ is the three-dimensional fluid velocity, $T(x, y, z, t)$ is the temperature, $p(x, y, z, t)$ is the fluid pressure, g is the (constant) acceleration due to gravity, $\widehat{\boldsymbol{z}}$ is a unit vector in the upward vertical direction, ν is the kinematic viscosity, a measure of the fluid's internal resistance to flow, and κ is the thermal diffusivity that measures the rate of heat conduction through the fluid (see the discussion of diffusion in the following section). Under the Boussinesq approximation, both ν and κ are assumed constant. Details of the derivation of the Navier–Stokes, continuity and heat advection-diffusion equations can be found in any good textbook on fluid dynamics – you might like to try Acheson (1990) if you're interested in finding out more; we will simply accept them as our starting point.

If the heating is not strong enough, the fluid does not convect, but simply conducts heat across the layer. The **conduction solution** is given by

$$\boldsymbol{u} = \boldsymbol{0}, \tag{1.5}$$

$$T = T_c(z) \equiv T_0 + \Delta T\left(1 - \frac{z}{d}\right), \tag{1.6}$$

$$p = p_c(z) \equiv p_0 - \int_0^z \rho(T_c(z))g \, \mathrm{d}z, \tag{1.7}$$

$$= p_0 - g\rho_0 z\left[1 - \alpha\Delta T\left(1 - \frac{z}{2d}\right)\right], \tag{1.8}$$

where p_0 is the pressure at the bottom of the layer, $z = 0$, and the pressure, $p_c(z)$, is the hydrostatic pressure of fluid in the conducting layer. (The hydrostatic pressure at a height z is the pressure due to the weight of fluid above z.)

When the fluid starts to convect, there will be departures from this conduction solution: to study these, we write $p = p_c(z) + \widehat{p}$ and $T = T_c(z) + \theta$. We also cast the equations into dimensionless form using the substitutions

$$(x, y, z) = d(\widetilde{x}, \widetilde{y}, \widetilde{z}), \tag{1.9}$$

$$t = \frac{d^2}{\kappa}\widetilde{t}, \tag{1.10}$$

$$\boldsymbol{u} = \frac{\kappa}{d}\widetilde{\boldsymbol{u}}, \tag{1.11}$$

$$\theta = \frac{\nu\kappa}{g\alpha d^3}\widetilde{\theta}, \tag{1.12}$$

$$\widehat{p} = \frac{\rho_0\nu\kappa}{d^2}\widetilde{p}. \tag{1.13}$$

The combination of these two sets of substitutions gives

$$\frac{1}{\sigma}\left(\frac{\partial\boldsymbol{u}}{\partial t} + (\boldsymbol{u}\cdot\nabla)\boldsymbol{u}\right) = -\nabla p + \theta\widehat{\boldsymbol{z}} + \nabla^2\boldsymbol{u}, \tag{1.14}$$

$$\frac{\partial\theta}{\partial t} + (\boldsymbol{u}\cdot\nabla)\theta - Ru_z = \nabla^2\theta, \tag{1.15}$$

where the tildes ($\tilde{}$) have been dropped immediately to simplify the notation, where u_z is the z-component of $\boldsymbol{u}$ and where $\sigma = \nu/\kappa$ is the **Prandtl number** that measures the relative effects of viscous and thermal diffusion, and

$$R = \frac{\alpha g d^3 \Delta T}{\kappa \nu} \tag{1.16}$$

is the **Rayleigh number** – the nondimensionalised version of the temperature difference between the top and bottom plates.

We now eliminate the pressure by taking the curl of equation (1.14) to get the vorticity equation

$$\frac{1}{\sigma}\left(\frac{\partial \boldsymbol{\omega}}{\partial t} + (\boldsymbol{u}\cdot\nabla)\boldsymbol{\omega} - \boldsymbol{\omega}\cdot\nabla\boldsymbol{u}\right) = \nabla\theta \times \widehat{\boldsymbol{z}} + \nabla^2\boldsymbol{\omega}, \tag{1.17}$$

where $\boldsymbol{\omega} = \nabla \times \boldsymbol{u}$ is the fluid vorticity.

To examine the stability of the conduction solution to convection we linearise equations (1.15) and (1.17) around $\boldsymbol{u} = \boldsymbol{\omega} = \boldsymbol{0}$, $\theta = 0$ giving

$$\frac{1}{\sigma}\frac{\partial \boldsymbol{\omega}}{\partial t} = \nabla\theta \times \widehat{\boldsymbol{z}} + \nabla^2\boldsymbol{\omega}, \tag{1.18}$$

$$\frac{\partial \theta}{\partial t} - R u_z = \nabla^2\theta. \tag{1.19}$$

Now acting on equation (1.18) with $\widehat{\boldsymbol{z}}\cdot\nabla\times$ gives

$$\frac{1}{\sigma}\frac{\partial}{\partial t}\nabla^2 u_z = \nabla_h^2\theta + \nabla^4 u_z, \tag{1.20}$$

where $\nabla_h = (\partial/\partial x, \partial/\partial y, 0)$ is the horizontal gradient operator.

We now need to solve equations (1.19) and (1.20) subject to suitable boundary conditions. The top and bottom plates are held at fixed temperatures, so the temperature perturbation θ must be zero there:

$$\theta = 0, \text{ at } z = 0, 1. \tag{1.21}$$

Mathematically, the simplest velocity boundary conditions to use are the so-called **stress-free** boundary conditions,

$$u_z = \frac{\partial^2 u_z}{\partial z^2} = 0, \text{ at } z = 0, 1, \tag{1.22}$$

that Rayleigh (1916) used in his calculation. We also assume that the convection cell is infinite in horizontal extent so that we do not have to consider any lateral boundary conditions. The solution can now be written as a superposition of Fourier eigenmodes

$$u_z^{(n)}(x, y, z, t) = u_n \sin n\pi z\, e^{i\boldsymbol{k}_h\cdot\boldsymbol{x}_h + st} + c.c., \tag{1.23}$$

$$\theta^{(n)}(x, y, z, t) = \theta_n \sin n\pi z\, e^{i\boldsymbol{k}_h\cdot\boldsymbol{x}_h + st} + c.c., \tag{1.24}$$